Article

Phase Risk Analysis of Overhead Lines Under Complex Icing Conditions

Xinsheng Dong [1,*], Yuanhao Wan [1], Yiran Zhang [2] and Yongcan Zhu [2,*]

1   Power Science Research Institute of State Grid Xinjiang Electric Power Co., Ltd., Urumqi 830011, China; 17690891895@163.com
2   School of Electronic Information, Xi'an Polytechnic University, Xi'an 710048, China; zhangyiran142723@163.com
*   Correspondence: dongxinsheng56@foxmail.com (X.D.); zhuyongcan@xpu.edu.cn (Y.Z.)

Abstract: Phase-to-ground discharge of transmission lines due to ice cover is a common issue. To assess the risk of phase-to-ground discharge of overhead lines under complex ice-covering conditions, this study used finite element analysis to model the interaction between ground wire, conductor, and insulator. The study examined how different factors affect the minimum safe distance between the conductor and ground wire, as well as the risk coefficient of phase-to-ground discharge and the risk zone. The finding reveals that as icing thickness increases, conductor bouncing intensifies, reducing the phase-to-ground distance, and placing one half of the line span within the risk zone for the given conditions. For the same length of de-icing, the closer the de-icing region is to the midpoint, the greater is the maximum jump height of the conductor. When the span is extended to 600 m, the risk range covers approximately 70% of the total line length. Under strong winds, conductor lateral displacement increases with wind speed, which leads to a higher risk of discharge.

Keywords: ground wire sag; overhead line; ice shedding; risk coefficient; risk interval

1. Introduction

Overhead transmission lines, a large channel for power transmission, frequently cross alpine mountainous areas and microtopographic regions, where prolonged ice formation is common. Typical issues, such as de-icing, conductor oscillations, flashovers, and structural faults, pose significant threats to the stability of lines [1]. Under severe ice conditions, single-phase tripping frequently results from reduced safety clearance between the conductor and ground line, resulting from sag or conductor bounce during de-icing [2]. For instance, in early November 2023, adverse weather in Xinjiang, China, including blizzards, gales, and sleet, caused multiple phase-to-ground tripping faults. Field observation and simulation identified ground wire sagging and conductor bounce during de-icing as key factors in reducing the safety clearance, as depicted in Figure 1.

Figure 1. Phase-to-ground discharge traces caused by the de-icing of transmission lines.

To mitigate the impact of ice on the safe and stable operation of overhead transmission lines, extensive research has been conducted globally on the dynamic response of lines to icing and de-icing loads, yielding useful results. For instance, Xinjiang Power Grid implemented measures such as adding spacer rods and increasing straight-line or tension tolerant towers to reduce stall distances in severely iced sections. However, these solutions are costly, time consuming, and limited by environmental factors in overhead line corridors. In a study, Zhang [3] analyzed changes in sag and de-icing bounce in an ultra-high voltage conductor, under uneven ice conditions but did not address conductor–ground line, safety distances, or discharge risk. A study conducted by Kong [4] proposed an overhead ground wire insulation program to prevent ice damage, by facilitating controlled ice melting and reducing mechanical stress. By contrast, Chen [5] proposed the "two factor ground wire breakage mechanism of increased tension due to ice cover" and decreased local mechanical strength due to discharge temperature rise and suggested modifying ground wire structures to prevent ice damage.

The risk of discharge due to de-icing jumps is more severe than the increased sag caused by ice accumulation. Justín Murín [6] used ANSYS software to create finite element models of a single conductor and a three-split conductor, simulating ice shedding at different positions. This study investigated the differences in dynamic response during ice shedding, focusing on jump height and tension variations between the single conductor and the three-split conductor. Kollár et al. [7] established a finite element model of transmission conductors using the finite element software ADINA and developed a scaled transmission line model. Through finite element simulations and experimental validation under actual conditions, they studied the ice shedding behavior of single conductors and double-split conductors. They also investigated the variations in jump height during ice shedding and the twisting angles of split conductors under different ice thicknesses, confirming the accuracy and reliability of the numerical model for the conductors. Fekr et al. [8] used the finite element software ADINA to establish finite element models of two-bundle transmission lines. They conducted in-depth studies on the effects of parameters such as ice thickness, span length, elevation difference, and ice shedding rate on ice jump behavior. Additionally, they performed detailed analyses of the dynamic response of conductors during ice shedding under various conditions through simulation. Wenjuan Lou et al. [9] studied the combined impact of wind and ice cover shedding on the jump height of iced conductors, analyzing the dynamic response of ultra-high voltage (UHV) transmission lines under such conditions through numerical simulation. The study proposed an empirical formula for the maximum jump height and verified its accuracy and applicability experimentally and through simulation data. Zhu Yongcan [10] analyzed the de-icing dynamic response under strong wind conditions using finite element analysis, discovering that strong wind increased and decreased longitudinal bounce height. This change might reduce the risk of phase-to-ground discharges while potentially increasing the risk of inter-phase discharges.

The above research provides a detailed analysis of the dynamic responses of overhead transmission lines under various operating conditions during ice shedding, including changes in jump height, lateral swing, and tension at certain typical locations on the conductor. However, there has been a lack of research on the changes in risk areas caused by ice shedding. In order to analyze single-phase discharge faults in transmission lines under icing conditions, this study established a finite element model of ice covered conductors and ground wires. It examined the variations in ground wire sag and conductor de-icing bounce height across different conditions, computed the changes in safety distance between the conductor and ground wire, and identified the most critical de-icing scenarios. This analysis provides theoretical support for understanding and mitigating phase-to-ground discharge faults in overhead lines under complex ice-covered conditions.

2. Analysis of Safety Distances for Overhead Line Conductors Under Ice-Covered Conditions

2.1. Transmission Line Space Structure

Phase-to-ground discharge faults in overhead lines due to ice accumulation are significantly influenced by conductor and ground wire spatial configurations. Currently, the

most common spatial arrangements for overhead transmission lines are the triangular and longitudinal layouts for their stability and efficiency under various environmental conditions. The triangular arrangement enhances stability by reducing oscillations during high winds, increases transmission capacity through optimized conductor spacing, and improves space efficiency by minimizing the required corridor width. However, attention must be given to the spacing between the ground wire and adjacent conductors during strong wind, heavy ice accumulation, and de-icing.

The longitudinal arrangement of the conductor–ground line reduces conductor-to-ground capacitance and enhances lightning resistance. However, during de-icing, the conductor's release of elastic potential energy causes it to spring upward, decreasing the distance to the nearest ground line and increasing the risk of discharge.

2.2. Safety Distance Analysis of Overhead Lines

When ice is abruptly removed from a transmission line, the tensioned line relaxes, causing the conductor to experience vertical displacement due to elastic potential energy and subsequently to oscillate. This alters the spacing between the conductor and ground lines. To assess the risk of phase-to-ground discharge post-de-icing, it is essential to calculate the minimum safe distance between the conductor and ground lines.

In triangular and longitudinal arrangements, the conductor and ground wire are positioned at an angle, not in the same vertical plane. However, during the de-icing jump, the conductor–ground line spacing decreases. When analyzing parallel transmission lines (ignoring crossing lines), the minimum clearance between phases and ground occurs when the conductors and ground wire are on the same horizontal plane. In Figure 2, S_1 represents the original conductor–ground line distance before de-icing, and S_2 denotes the significantly reduced spacing after de-icing.
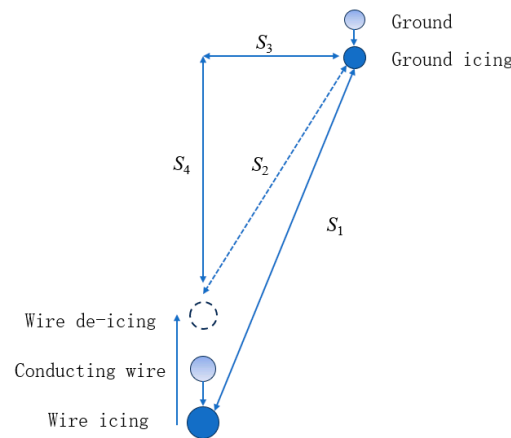

Figure 2. Changes in the spacing of ground conductors after de-icing.

By extracting the spatial coordinates of each point on the ground wires at different moments, the minimum distance between the ground wires can be calculated using the Pythagorean theorem. The expression for the minimum distance between ground wires is as follows:

$$S_2 = \sqrt{S_3^2 + S_4^2} \tag{1}$$

3. Finite Element-Based Analytical Model of Phase-to-Ground Line Spacing for Ice-Covered Lines

3.1. Ground Arc Pendant Modeling and Solution Methods

3.1.1. Calculation of the Sag of the Conductor–Ground Line

The shape of the overhead conductor and ground line, as shown in Figure 3, is often described using a hanging chain model. In the catenary model of the transmission line, the conductor regarded as an ideal flexible cable is subjected to a uniformly distributed load

across the diagonal span. A coordinate system is defined with the lower suspension point A as the origin, the *x*-axis perpendicular to the specific load, and the *y*-axis parallel to the specific load. Subsequently, the oblique parabolic equation of the overhead transmission line is derived as follows:
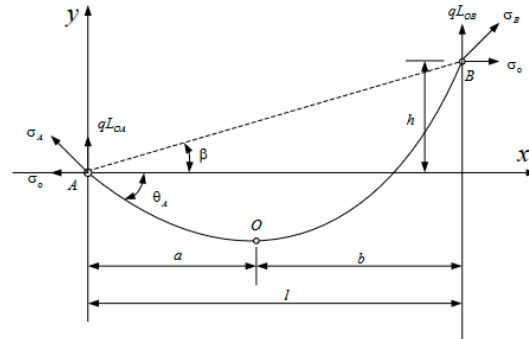

Figure 3. The force diagram of a transmission line with two suspension points at different heights.

When the two suspension points are at different heights, it is usually assumed for calculation purposes that the left suspension point A is at the origin. The horizontal distance from the lowest point O to the left suspension point is a, and the horizontal distance to the right suspension point B is b.

When the two suspension points are at the same height, the length of the entire span is the following:

$$L_{h=0} = 2\frac{\sigma_o}{q}\sinh\frac{lq}{2\sigma_o} \tag{2}$$

The equation of the catenary is as follows:

$$y = \frac{h}{L_{h=0}}\left[\frac{2\sigma_o}{q}\sinh\frac{qx}{2\sigma_o}\cosh\frac{q(l-x)}{2\sigma_o}\right] - \sqrt{1+(\frac{h}{L_{h=0}})^2}\left[\frac{2\sigma_o}{q}\sinh\frac{qx}{2\sigma_o}\sinh\frac{q(l-x)}{2\sigma_o}\right] \tag{3}$$

The sag f_x at any point C in the overhead line stall is:

$$f_x = \frac{h}{l}x - \frac{h}{L_{h=0}}\left[\frac{2\sigma_o}{q}\sinh\frac{qx}{2\sigma_o}\cosh\frac{q(l-x)}{2\sigma_o}\right] + \sqrt{1+(\frac{h}{L_{h=0}})^2}\left[\frac{2\sigma_o}{q}\sinh\frac{qx}{2\sigma_o}\sinh\frac{q(l-x)}{2\sigma_o}\right] \tag{4}$$

In the equation, *h* represents the height difference of the conductor in meters (m); *q* denotes the unit load; *x* is the horizontal coordinate of the selected point; *l* is the span length of the conductor in meters (m); $L_{h=0}$ indicates the length of the entire span when the two suspension points are at the same height, measured in meters (m); and σ_o represents the horizontal component of the stress at various points along the transmission line.

The hanging chain line equation accurately calculates conductor sag and is widely used. However, it becomes ineffective under complex working conditions such as uneven ice accumulation and strong winds.

3.1.2. Nonlinear Finite Element Method

Transmission line shape determination using the finite element method is a common approach to calculate the prestress distribution and geometry of the conductor and ground wires. By setting initial shapes and stresses, an iterative process is used to approximate an accurate solution. The horizontal tension and displacement at the lowest point serve as convergence criteria to ensure accuracy and stability. To expedite convergence, a reduced elastic modulus (about 1×10^{-3} order of magnitude) is utilized during shape-finding, which is restored to the true value of subsequent static and dynamic analyses.

The conductor model LGJ-630/45 and the ground wire model OPGW-185 are used, with the basic parameters listed in Table 1. For a span of 400 m, the conductor's sag is compared between the suspended chain calculation (Equation (4)) and the finite element simulation, as shown in Figure 4. The line in Figure 4 represents the error between the theoretical calculation values and the finite element simulation results. The difference between the computed and simulated values is minimal, with an error margin within 0.2% and a minimum of 0.028%. This confirms that the nonlinear finite element model accurately predicts the sag of overhead transmission lines.

Table 1. Ground wire models.

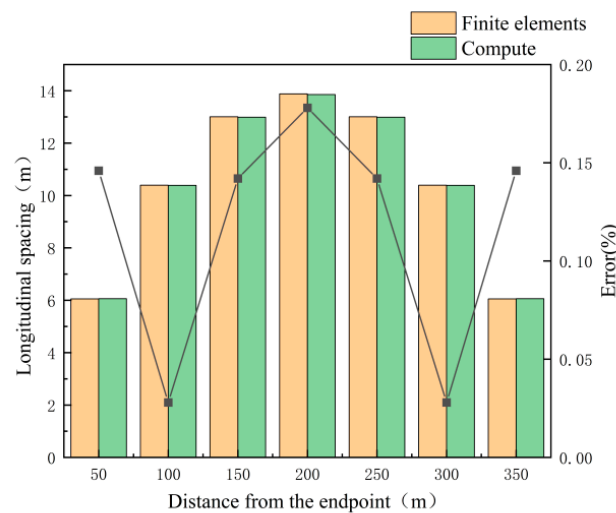| Model	Diameter/m	Cross-Sectional Area/m^2	Weight/(kg/km)	Elastic Modulus/GPa
LGJ-630/45	33.6×10^{-3}	666.55×10^{-6}	2060	63
OPGW-185	18.2×10^{-3}	184.38×10^{-6}	1071	132

Figure 4. Calibration diagram of sag value.

3.2. Analytical Modeling of the Dynamic Response of Conductor De-Icing Bouncing

This article uses the aforementioned calculation method for conductor sag to establish a three-dimensional finite element model of a five-section ground wire. The conductor is modeled using the Link 10 element, which is a 3D bar element that can only endure axial forces, either in tension or compression, and can be used to simulate cables or gaps. The insulator string is simplified as a bar and modeled with the Link 8 element, a bar element with properties suitable for large deformations and stress stiffening.

Conductor de-icing involves complex energy conversion and equilibrium processes. When ice forms on a conductor, it stores additional gravitational potential energy and elastic potential energy [11]. As environmental conditions change such as temperature rise or other external forces, the ice may suddenly detach, releasing the stored elastic energy, which is transformed into kinetic and new potential energy of the conductor, causing the conductor to oscillate. The vibration gradually diminishes due to air resistance, wire self-damping, and insulator string inertia, until the conductor stabilizes, simplifying the process into a basic mechanical model [12]:

$$M\ddot{v} + C\dot{v} + Kv = F(a) \tag{5}$$

where M represents mass matrix; C denotes damping matrix, K signifies stiffness matrix; $\ddot{v}$ refers to acceleration; $\dot{v}$ represents velocity; v is displacement; and F(a) denotes the external force vector.

3.3. Calculation of Ice and Wind Loads on Conductors

3.3.1. Ice Cover Load and De-Icing

Ice cover increases the pressure of overhead lines and alters their mechanical properties. The cross-sectional shape and characteristics of the ice are influenced by factors such as climate, ice purity, and structural properties. For practical engineering estimates, a simplified approach assumes uniform ice distribution along the conductor. Figure 5 illustrates a schematic of the ice-covered conductor cross-section.
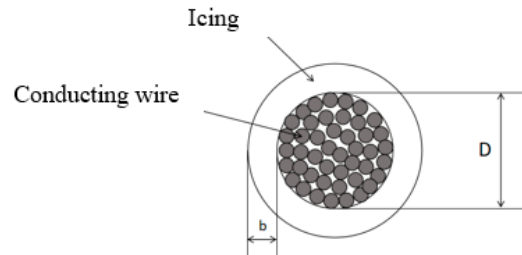

Figure 5. Cross-section of the iced conductor.

The additional force simulation method models ice loading by applying equally spaced concentrated forces, where the mass M of each concentrated load is determined as follows:

$$\begin{cases} m = \rho \pi b (D + b) \\ M = mgL/n \end{cases} \tag{6}$$

where m denotes the mass per unit length of the ice cover on the conductor (kg/m); ρ and b represent the ice cover's density (900 kg/m^3) and thickness (mm), respectively; D and L refer to the wire's outer diameter (mm) and length (m), respectively; g is the acceleration of gravity (9.8 N/kg); n represents the number of dividing units. In order to simplify the problem, this paper set the de-icing time to 0.02 s in the simulation and used the method of sudden load withdrawal to simulate the shedding process of the overlying ice.

3.3.2. Wind Load

Given the large stall distance and complex structure of overhead lines, load size varies due to differences in component structure and location. When the angle θ degree between the guide line's axial direction and the horizontal direction is considered, the wind pressure acting orthogonally to the unit length of the guide line is referred to as horizontal wind load L_n (N/m). Due to the complexity of wind loads in real-world environments, various factors need to be considered when calculating wind loads [13,14]. The airflow carries kinetic energy, which is converted into static pressure, or velocity pressure, forming part of the air pressure in the Bernoulli equation. This calculation yields the baseline wind pressure. Additionally, it is essential to consider the effects of span length, wind direction, and surface roughness on wind speed. Horizontal wind load per unit L_n (N/m) and specific load γ_n (N/m) are computed as follows:

(1) Without icing

$$L_n = W_o D \alpha \beta_c \mu_{sc} \mu_s \mu_\theta \times 10^{-3} \tag{7}$$

$$\gamma_n = \frac{L_n}{A} \tag{8}$$

(2) Icing

$$L_y = W_o (D + 2b) \alpha \beta_c \mu_{sc} \mu_s \mu_\theta \times 10^{-3} \tag{9}$$

$$\gamma_y = \frac{L_y}{A} \tag{10}$$

where W_o denotes the standard value of reference wind pressure, with $W_o = \frac{V^2}{1.6}$, N/m^2; α signifies the unevenness coefficient of wind pressure; β_c: represents 500 kV line conductor wind load adjustment factor; μ_{sc} refers to conductor–ground wire body shape factor; μ_s is the coefficient of variation of wind pressure height; μ_θ denotes the coefficient of variation of wind pressure with wind direction due to the angle between the wind direction and the axis of the guide line, $\mu_\theta = \sin^2 \theta$.

4. Analysis of Discharge Risk Coefficients of Overhead Conductors Under Different Icing Conditions

4.1. Definition of the Risk Factor for Discharge of Overhead Conductors Under Ice-Covered Conditions

The conductor–ground line safety distance is the minimum separation required in a power system to prevent flashover or breakdown between the conductor and the ground line. If the distance is exceeded, the overhead line is at risk of severe failure.

According to the 110–750 kV overhead transmission line design technical regulations [15], a 500 kV line conductor discharges at a minimum gap of 1.3 m. Due to the formation of ice ridges on the surface of the ground wire caused by icing or other abnormal weather conditions, and considering that the calculation results of this model may be affected by factors such as the damping coefficient, it is important to avoid accidents in actual engineering. Therefore, to increase the margin of safety, the minimum distance is expanded to 2 m. This means that if the distance between the ground wire and other elements is less than or equal to 2 m, it is considered to be within the risk range.

To simplify the analysis, this study assessed the risk of phase-to-ground discharge in overhead lines by comparing the minimum distance between the ground and conductor under de-icing conditions. The risk of phase-to-ground discharge is inversely proportional to the distance. The phase-to-ground discharge risk coefficient W of the line is calculated as follows:

$$W = \frac{L_1}{D_1} \tag{11}$$

where L_1 represents the minimum safe distance of the conductor–ground line (m); D_1 denotes the minimum distance of the conductor–ground line under the ice-covered load and de-icing condition (m). A larger value of W signifies a greater risk of phase-to-ground discharge.

According to the study in [16], when the de-icing span count changes in mid-span, the constraint on both ends of the conductors in isolated spans is more uniformly sufficient. This results in significantly lower de-icing jump heights for isolated spans under icing conditions compared to continuous spans. As the number of continuous spans increases, the de-icing jump height gradually increases; however, when the span count exceeds five, the jump height almost no longer increases. Therefore, a continuous span configuration of five spans is more practical.

Assuming a transmission line with five consecutive sections, where only the central section's conductor is de-iced, the conductor is LGJ-630/45 and the ground wire is OPGW-185, with a voltage level of 500 kV. The initial longitudinal distance without ice cover is 13 m, and the safety distance is 2 m. Model parameters include a de-icing section length of 400 m, divided into 400 grids, with no height difference and 100% de-icing. The conductor–ground line bounce diagram for a 30 mm ice cover is shown in Figure 6. The intersection of purple and green represents the scenario where the de-icing jump of the iced conductor occurs at the same vertical plane position as the iced ground wire. Due to the fact that the bouncing conductor and ground wires are not on the same vertical plane in spatial modeling (as shown in Figure 2), the minimum distance of 2 m between the ground wire and the conductor corresponds to a horizontal distance of 2 m. Therefore, when the vertical distance between the two wires coincides, it falls within the risk zone.
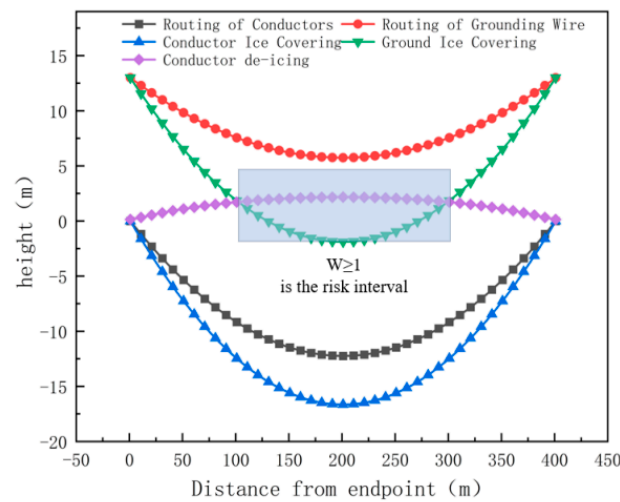
Figure 6. Schematic diagram of 30 mm icing thickness and de-icing bounce of the ground conductor.

For a continuously ice-covered overhead line with no height variation, experience indicates that the risk of phase-to-ground discharge is greatest at the midpoint of the span and decreases toward the endpoints. The phase-to-ground discharge risk coefficient W is highest at the midpoint. The risk area for phase-to-ground discharge can be determined by calculating W at each grid point. For a 30 mm ice cover, the vertical sag of the conductor's lowest point is 16.646 m, while that of the ground line is 14.888 m. The maximum conductor bounce height is 18.815 m. The minimum conductor–ground line distance of 2 m or less defines the risk area, which spans 102–298 m and constitutes 49% of the total line length.

4.2. Impact of Ice Cover Thickness on Discharge Risk

Assuming a transmission line with five consecutive sections, where only the middle section's conductor is de-iced, the model parameters are as follows: a de-icing span of 400 m, divided into 400 grids, no height variation, an initial conductor tension of 29,740 N, and initial ground line tension of 21,000 N. Using 100% de-icing, simulations are performed with ice cover thicknesses of 10, 15, 20, 25, and 30 mm. The maximum sag of the conductor–ground line and the maximum height of the conductor's ice bounce are calculated, with the minimum spacing between the conductor and ground line detailed in Table 2.

Table 2. Effect of different icing thickness on the safety distance of the ground conductor.

Ice Thickness/mm	Maximum Sag of the Conductor Wire/m	The Maximum Sag of the Wire/m	The Maximum Jump Height of the Wire/m	Minimum Spacing Between Ground and Conductor Wires/m
No icing	10.221	13.878	/	15.150
10	11.503	14.634	7.252	9.101
15	12.299	15.091	10.634	5.532
20	13.143	15.584	13.671	2.670
25	14.011	16.105	16.381	2.000
30	14.888	16.646	18.815	2.000

As the ice cover thickness increases, the conductor's sag also rises. When the thickness increases from 10 to 30 mm, the conductor's maximum jump height grows by 259%, and the minimum conductor–ground distance decreases from 9.101 to 2 m, reaching the safety distance and impacting the transmission line's operation. A risk is defined when $W \geq 1$. The phase-to-ground discharge risk factor decreases from the midpoint toward the insulator. The closest grid point where $W \geq 1$ is defined to determine the risk section. With 400 grid per span, the corresponding intervals were plotted as in Figure 7.
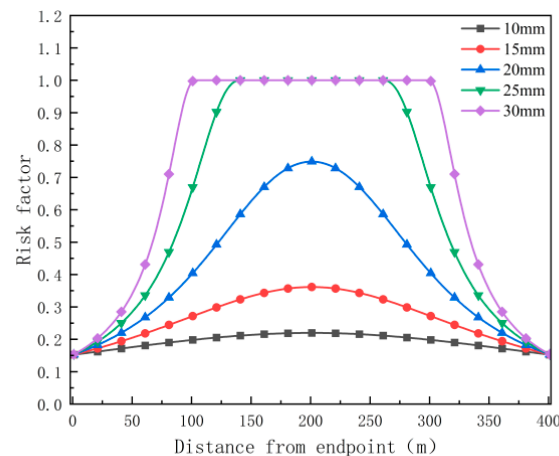
Figure 7. Risk range of wire de-icing and bounce under different icing thicknesses.

Increased ice thickness on the line leads to greater conversion of gravitational potential energy into elastic potential energy during de-icing, resulting in higher bounce heights. As shown in Figure 7, for ice thicknesses of 10, 15, and 20 mm, the danger zone is minimal, nearly zero. For 25 mm ice cover, the risk zone spans 140–260 m, about 30% of the total line length. With 30 mm ice cover, the risk zone expands to 49% of the line length, significantly increasing the risk of conductor–ground flashover. Inclement weather, such as rain and snow, exacerbates this risk, potentially disrupting transmission line operations. Therefore, additional protective measures should be considered for affected sections.

4.3. Effect of Uneven Ice Cover on the Safety Distance of Conductor–Ground Wires

In practice, ice coverage is often uneven along the line, leading to potential variation in the arc droop, which may not occur at the mid-point if there is no height difference. To simulate uneven ice cover, finite element analysis is used with different point loads applied to the line. For a 40 mm ice thickness in specific areas and 30 mm elsewhere, the overhead line is divided into 400 grids with measurements taken every 50 grids totaling eight points. Adjustments to the ice-covered area are illustrated in Figure 8 for the single-file line ice-covering model.
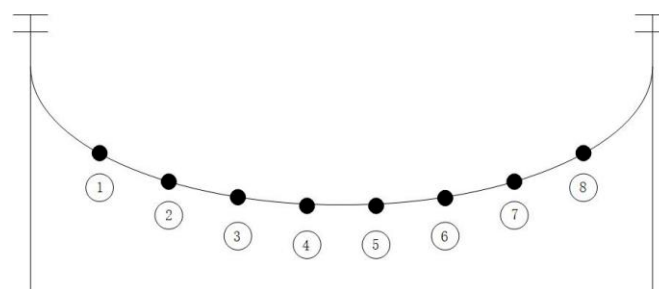

Figure 8. Icing model of the single-gear line.

Due to the transmission line's symmetry, only the midpoint of one side is analyzed for varying ice cover scenarios. The analysis sequentially examines ice concentrations at locations ①②, ②③, ③④, and ④⑤, focusing on changes in the safety distance between the conductor and ground line and variation discharge intervals. The results are presented in Tables 3 and 4.

Table 3. Effect of the safety distance of the ground conductor.

The Type of Scenario	Maximum Sag of the Conductor Wire/m	The Maximum Sag of the Wire/m	Maximum Sag Position	The Maximum Jump Height of the Wire/m	Minimum Spacing Between Ground and Conductor Wires/m	Phase-to-Ground Discharge Risk Factor
①②	15.408	17.124	195	19.597		
②③	16.184	17.729	190	20.548	2.000	1.000
③④	16.946	18.38	189	21.586		
④⑤	17.253	18.684	200	22.187		

Table 4. Risk range of de-icing and bounce of uneven iced wires.

The Type of Scenario	Risk Range
①②	89–308
②③	82–314
③④	83–315
④⑤	85–315

Uneven ice cover has a notable impact on transmission lines. When heavy ice is near the conductor's midpoint, the maximum sag of the conductor and earth wire decreases, and the sag shifts accordingly. With heavy ice at the symmetrical midpoint, the sag is maximized, and the conductor can bounce up to 22.187 m. The minimum conductor–ground distance remains at 2 m, resulting in a phase-to-ground discharge risk coefficient of 1, indicating high risk. When heavy ice is near the insulator, the risk zone increases to about 55%, with the area near the midpoint rising to approximately 58%, concentrated between 83 and 315 m. Compared with uniform ice cover, this results in an expanded risk zone. Therefore, to mitigate risks, measures should be taken to reduce ice accumulation in the conductor's central area during operation.

4.4. Effect of Uneven De-Icing on Safety Distances

External factors, such as temperature and wind direction combined with the structural characteristics of transmission lines, can lead to localized de-icing. This localized de-icing causes oscillations and complicates the line due to the traction effect of the de-iced area. Using finite element simulation, this study modeled uneven de-icing by sequentially removing ice loads from various sections, adjusting de-icing positions, and analyzing changes in parameters and risk intervals (Tables 5 and 6).

Table 5. Effect of uneven de-icing on the safety distance of the ground conductor.

De-Icing Area	Maximum Sag of the Conductor Wire/m	The Maximum Sag of the Wire/m	The Maximum Jump Height of the Wire/m	Minimum Spacing Between Ground and Conductor Wires/m	Phase-to-Ground Discharge Risk Factor
①–③			5.455	9.262	0.216
①–④			8.837	6.185	0.323
②–⑤	14.888	16.646	12.224	3.227	0.620
③–⑥			13.380	2.429	0.823
①–⑤			12.931	2.708	0.739
①–⑥			16.140	2.000	1.000

Table 6. Risk range of de-icing and bouncing of uneven iced wires.

De-Icing Area	Risk Range
①–③	None
①–④	None
②–⑤	None
③–⑥	None
①–⑤	None
①–⑥	141–256

The de-icing area of the conductor does not affect the maximum sag of the ground line. Due to energy conservation, the maximum sag of the conductor also remains constant. As the de-icing area increases from 150 to 300 m, the conductor's bounce height rises from 5.455 to

16.140 m, and the minimum spacing between the conductor and ground line decreases from 9.262 to 2 m. At 300 m de-icing, a risk zone of 115 m (accounting for 28.75% of the total length of the line) emerges, concentrated on the left side of the line. When de-icing occurs under other conditions, if the minimum spacing of the guide wire is 2.708 m, there is no discharge risk. Generally, a de-icing area closer to the line results in a higher bounce height and a smaller minimum spacing of the guide wire.

4.5. Influence of Overhead Line Structure on Safety Distances

The safety distance of the guide line is crucial for ensuring the safe operation of power lines. A smaller pitch results in a tauter guide wire with reduced sag, thereby maintaining a larger safety distance. However, this change also increases tower quantity, construction cost, and maintenance complexity. Conversely, a larger pitch causes the guide wire to sag more, potentially reducing the safety distance. By varying the pitch, we analyzed the maximum sag, conductor jump height and the risk interval for 30 mm of ice cover. The results are summarized in Table 7 and Figure 9. Each experiment required recalculating the static sag without ice cover due to changes in pitch.

Table 7. The influence of different gear distances on the safety distance of the ground conductor.

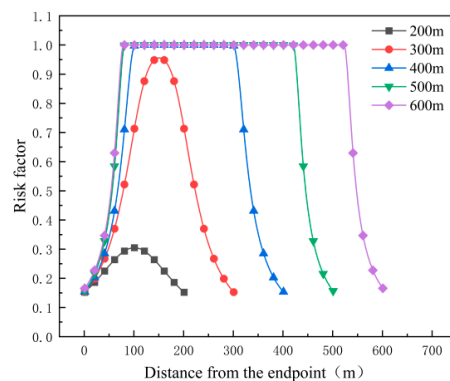| Pitch/m	Maximum Sag of the Conductor Wire/m	The Maximum Sag of the Wire/m	Wire De-Icing Jump Height/m	Minimum Spacing Between Ground and Conductor Wires/m	Phase-to-Ground Discharge Risk Factor
200	5.475	5.176	6.456	6.557	0.305
300	10.506	10.141	12.020	2.093	0.956
400	14.188	16.646	18.815	2.000	1.000
500	21.992	24.760	26.429	2.000	1.000
600	29.156	34.551	33.264	2.000	1.000

Figure 9. Risk range of de-icing and bounce of wires with different pitches.

As the gear distance increased from 200 to 600 m, both the maximum sag of the ground and the conductor rose, peaking at 29.156 and 34.551 m, respectively. The conductor's de-icing bounce height grew from 6 to 33 m, an increase of 27 m. For gear distances of 200 and 300 m, the minimum distance between the conductor and the ground line exceeded the safe distance of 2 m, with a risk coefficient of less than 1, indicating no risk. However, at a gear distance from 400 to 600 m, the conductor's bounce height surpassed the lowest point of the ice-covered ground line, reducing the minimum distance between the conductor and the ground line to 2 m, with a risk coefficient of 1. Consequently, the risk zone expanded from the 197 m range to 442 m, with the 600 m gear distance resulting in a risk area of 73.667%. Therefore, during installation, selecting an appropriate gear distance is crucial to mitigate risk expansion.

4.6. Impact of Strong Winds on Safety Distances for Conductors

Strong winds can induce oscillations in lead wires, potentially leading to contact or collision between them. The wind load on the wires causes these oscillations, influenced by the wind speed, direction, and the wire's shape, size, and suspension. Wind speeds of 10,

15, 20, 25, and 30 m/s are considered, with wind direction perpendicular to the wire axis, as illustrated in Figure 10.
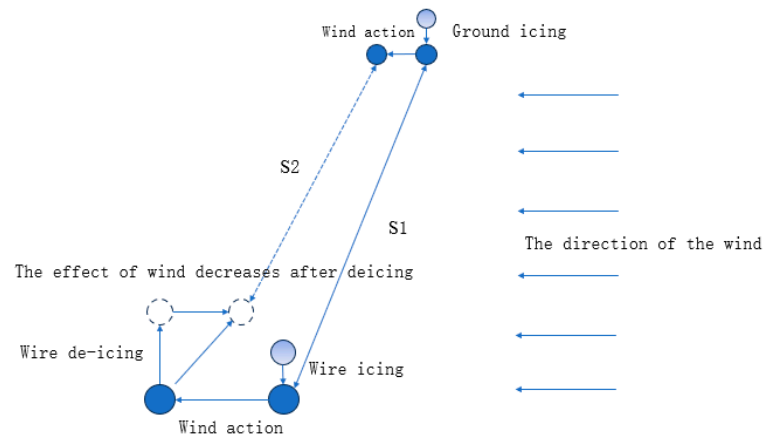

Figure 10. Schematic diagram of the displacement of the conductor after de-icing under strong winds.

The maximum sag of the conductor and earth wire along with the lateral and longitudinal displacements after de-icing and the discharge risk interval were analyzed for various wind speeds (Tables 8 and 9). Figure 11 illustrates a time course diagram of conductor displacement at different wind speeds.

Table 8. Analysis of the safety distance of the ground conductor at different wind speeds.

Wind Velocity/(m/s)	Maximum Sag of the Conductor Wire/m	The Maximum Sag of the Wire/m	The Horizontal Distance of the Ground Wire/m	Maximum Longitudinal Displacement of the Wire After De-Icing/m	Maximum Lateral Displacement of the Conductor After De-Icing/m	Minimum Spacing Between Ground and Conductor Wires/m	Phase-to-Ground Discharge Risk Factor
5	14.876	16.636	1.933	18.810	0.675	1.710	1.170
10	14.701	16.492	1.734	18.689	2.678	1.512	1.323
15	14.010	15.907	1.483	18.191	5.842	2.460	0.813
20	12.781	14.809	1.340	17.261	9.150	4.899	0.408
25	10.881	12.966	1.336	15.679	12.816	7.459	0.268

Table 9. The risk range of traverse de-icing and bounce at different wind speeds.

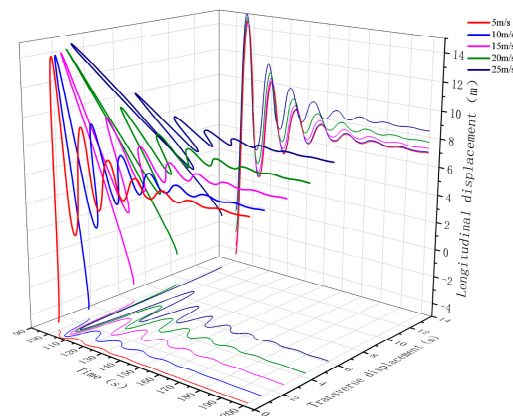| Type of Working Condition	Risk Interval
5 m/s	90–314
10 m/s	84–320
15 m/s	None
20 m/s	None
25 m/s	None

Figure 11. Time history of traverse displacement at different wind speeds.

As wind speed increases, both the sag of the earth wire and conductor decreases. With wind perpendicular to the conductor axis, the horizontal distance between the conductor and the ground line diminishes. At 25 m/s wind speed, this distance reaches a minimum of 1.336 m. Increasing wind speed from 5 to 25 m/s reduces the maximum longitudinal displacement of the de-iced conductor by approximately 3 m, while the maximum transverse displacement increases by 0.675–12.816 m.

Consequently, the vertical separation between the conductor and the ground line decreases, reducing the sag. Since the conductor and ground are on different horizontal planes, analyzing only the midpoint of the conductor is inadequate for assessing the minimum spacing between them. A comprehensive analysis is required due to the spatial nature of de-icing bounce. At wind speeds of 5 and 10 m/s, the minimum distance between the conductor and the ground line falls below the safety threshold, with phase-to-ground discharge risk coefficients exceeding 1 (ranging from 1.170 to 1.323), thereby increasing the risk of discharge. At 5 m/s, discharge occurs 56% of the time, rising to 59% when the wind speed is 10 m/s. Lower wind speed results in smaller horizontal displacements, heightening the risk of discharge during de-icing. Excessive wind speeds, however, cause significant horizontal displacement of the earth wire relative to the conductor, paradoxically increasing the conductor-to-ground distance and reducing discharge risk.

5. Conclusions

In this study, the risk of phase-to-ground discharge of overhead lines under complex ice-covering conditions was analyzed in depth, in order to provide a theoretical basis for fault prevention and treatment. The finite element model of overhead lines was established, and the influence of different conditions on the discharge coefficient of the conductor–ground line of the overhead line and the discharge interval was studied. The following conclusions were drawn:

The thickness of ice cover increases, the arc droop of the earth wire and the height of the conductor's de-icing jump increases significantly, the phase-to-ground distance decreases, and the phase-to-phase discharge coefficient appears to be equal to 1 when the thickness of ice cover reaches 20 mm. Especially when the thickness of ice cover reaches 30 mm, the risk interval expands to 49% of the total length of the line.

Uneven ice cover leads to uneven local load of the overhead line, resulting in individual parts of the sag abnormally increasing, but also making the lowest sag position deviate from the middle point of the wire, and with the heavy ice cover position closer to the middle point of the wire, the greater is the risk area at close to 57%

Uneven de-icing caused by local vibration of the conductor, line side of the de-icing and de-icing area, is 300 m long when there is a discharge risk section—the section for the middle of the side near the de-icing area, accounting for 28.75% of the total length of the line.

The cumulative effect of the long gear distance caused by the growth of the arc of the conductor and ground line after icing is more prominent—the gear distance increased from 200 m to 600 m, the increase in the arc of the conductor reached 19.4 m, the arc of the ground line increased to 23.7 m; the 600 m gear distance of the conductor de-icing bouncing risk area is as high as 73.667%.

In strong wind conditions, the wind causes the arc droop of the conductor to decrease, the discharge easily occurs when the wind speed is small, and the horizontal displacement of the conductor increases while the risk of discharge decreases with larger wind speeds.

This paper analyzed the risk zones between the conductors and the ground wire under different operating conditions, drawing several conclusions beneficial to engineering design. However, there was limited consideration of discharge risks between the conductors and ground wire in cases involving special terrains or split conductors.

References

1. Zhang, Y.; Guo, Y.; Lou, W.; Zhou, W.; Huang, M. Dynamic response of a transmission conductor following delayed ice shedding by reduced-scale model test. *Cold Reg. Sci. Technol.* **2024**, *226*, 104288. [CrossRef]
2. Zhang, Z.; Zhang, H.; Yue, S.; Zeng, W. A Review of Icing and Anti-Icing Technology for Transmission Lines. *Energies* **2023**, *16*, 601. [CrossRef]
3. Zhang, J.; Zhang, Y.; Wang, J.; Chu, Z.; Sun, Q.; Zhou, W.; Jiang, Y. Research on Uneven Iced Transmission Lines and the Dynamic Response after Ice-shedding. *Chin. J. Appl. Mech.* **2023**, *40*, 558–570.
4. Kong, X.; Fang, Y.; Zhao, J.; Jiang, D. Research on the Scheme of Overhead Ground Wire Lightning Protection and Melting-ice System. *High Volt. Appar.* **2021**, *57*, 154–161.
5. Chen, Y.; Fan, S.; Wang, X.; Yu, J.; Song, P.; Lu, Y. Anti-icing Technology for Transmission Lines Based on New Ground Wire Structures and Operation Modes. *High Volt. Eng.* **2024**, 1–10. [CrossRef]
6. Murín, J.; Hrabovský, J.; Gogola, R.; Janíček, F. Dynamic Analysis of Overhead Power Lines after Ice-Shedding Using Finite Element Method. *J. Electr. Eng.* **2016**, *67*, 421–426. [CrossRef]
7. Kollár, L.E. Dynamics of digitally controlled forced vibration of suspended cables. *Meccanica* **2023**, *58*, 25–42. [CrossRef]
8. Fekr, M.R.; Mcclure, G. Numerical modelling of the dynamic response of ice-shedding on electrical transmission lines. *Atmos. Res.* **1998**, *46*, 1–11. [CrossRef]
9. Lou, W.-J.; Zhang, Y.-L.; Xu, H.-W.; Huang, M.-F. Jump height of an iced transmission conductor considering joint action of ice-shedding and wind. *Cold Reg. Sci. Technol.* **2022**, *199*, 103576. [CrossRef]
10. Zhu, Y.; Xie, S.; Dong, X.; Shu, X.; Wang, S.; Zhang, Y. Research of Ice-shedding Response of Transmission Lines Under Strong Winds. *Power Syst. Technol.* **2024**, *48*, 1779–1787.
11. Dong, X.; Zhao, M.; Li, M.; Zhu, Y. Study on the Bouncing Process Induced by Ice Shedding on Overhead Conductors under Strong Wind Conditions. *Appl. Sci.* **2024**, *14*, 4285. [CrossRef]
12. Xu, G. *Numerical Simulation Study of Iced Conductor on Dynamic Response of Ice-Shedding on Transmission Lines*; Xi'an Polytechnic University: Xi'an, China, 2016.
13. *DL/T5154-2012*; Technical Regulations for Design of Tower Structures of Overhead Transmission Lines. Available online: https://www.chinesestandard.net/PDF/English.aspx/DLT5154-2012 (accessed on 15 November 2024).
14. Shao, T. *Mechanical Calculation of Overhead Power Transmission Lines*; China Electric Power Press: Beijing, China, 2003.
15. Zhang, Y.; Jiang, Y.; Li, X.; Zhou, W.; Tan, H.; Zhang, X.; Sun, Q. Calculation of jump height for uneven ice-shedding of overhead transmission lines. *J. Vib. Shock.* **2023**, *42*, 75–86.
16. *DL/T 5485-2013*; Technical Code for Design of Long Span Crossing of 110 kV~750 kV Overhead Transmission Line. Available online: https://www.chinesestandard.net/PDF/English.aspx/DLT5485-2013 (accessed on 15 November 2024).